JOURNAL OF SOLID STATE CHEMISTRY 119, 115–119 (1995)

Crystal Structure of the High-T_c Superconductor $HoSr_2Cu_{2.7}Mo_{0.3}O_{7.54}$ by Joint Time-of-Flight Neutron/X-Ray Rietveld Refinement

William T. A. Harrison, Stan Roliard, John T. Vaughey,[1] Lumei Liu, and Allan J. Jacobson

Department of Chemistry and Texas Center for Superconductivity, University of Houston, Houston, Texas 77204-5641

Received May 4, 1995; in revised form May 31, 1995; accepted June 14, 1995

The ambient-pressure synthesis, crystal structure, and some properties of $HoSr_2Cu_{2.7}Mo_{0.3}O_{7.54}$ are described. $HoSr_2Cu_{2.7}Mo_{0.3}O_{7.54}$ crystallizes as the tetragonal modification of the $YBa_2Cu_3O_{7-\delta}$ (123) high-T_c superconductor structure, and exhibits a superconducting transition temperature of ~30 K. The Cu/Mo cation distribution in $HoSr_2Cu_{2.7}Mo_{0.3}O_{7.54}$ was established by means of a joint time-of-flight neutron/X-ray Rietveld refinement: The molybdenum ions substitute for copper at both the "chain" [Cu(1)] and square-pyramidal [Cu(2)] sites in roughly equal proportion. The chain layers [atoms Cu/Mo(1) and O(1)] show considerable static disorder in this material. Crystal data: $HoSr_2Cu_{2.7}Mo_{0.3}O_{7.54}$, M_r = 660.51, tetragonal, space group *P4/mmm* (No. 123), a = 3.83107(6) Å, c = 11.5347(3) Å, V = 169.296(8) Å^3, Z = 1, R_p = 4.21%, R_{wp} = 5.08%, and χ^2 = 2.45. © 1995 Academic Press, Inc.

INTRODUCTION

Pure $YSr_2Cu_3O_7$ (1), the strontium-containing counterpart to the T_c = ~95 K "123" superconductor $YBa_2Cu_3O_{7-\delta}$, may only be prepared at very high pressures, in excess of 6 GPa (1). The same situation applies when most of the lanthanide cations are substituted for yttrium (2). However, these phases may be prepared at ambient pressure when a small percentage of copper is replaced by one of several other cations (3), as $YSr_2Cu_{3-x}M_xO_{7\pm\delta}$ (M = Pb, Li, Al, Ti, V, Cr, Fe, Co, Ga, Ge, Mo, W; $x \approx 0.3$ in most cases). This doping may occur at one or both of the two distinct copper sites: the "chain" site [here denoted Cu(1)], or the square-pyramidal, or "planar" site [Cu(2)]. Because the superconducting behavior of these systems critically depends on the precise composition and geometry of the copper-containing layers, high-quality structural data are essential in furthering our understanding of these unusual materials.

The crystal structure of $YSr_2Cu_{2.7}Mo_{0.3}O_7$, based on powder X-ray diffraction and electron microscopy measurements, was reported by Hu *et al.* (4). These workers found that the majority of molybdenum substitution (~24%) in $YSr_2Cu_{2.7}Mo_{0.3}O_7$ occurs at the square-pyramidal Cu(2) site, with only ~6% Mo substitution for copper at the chain site, Cu(1). However, when Harlow *et al.* (5) studied $YSr_2Cu_{3-x}M_xO_{7+\delta}$ (M = Mo, W, Re) by single crystal X-ray and powder neutron methods, their conclusion was the opposite: that Mo substitutes largely at the chain [Cu(1)] site in $YSr_2Cu_{3-x}Mo_xO_{7+\delta}$.

In this paper we describe the detailed crystal structure of $HoSr_2Cu_{2.7}Mo_{0.3}O_{7.54}$, as determined by a joint neutron/X-ray profile refinement: In this phase, Mo shows little site preference for the two Cu sites. The Mo-doped Cu(1)/O(1) layers in $HoSr_2Cu_{2.7}Mo_{0.3}O_{7.54}$ show considerable disorder, similar to the effect seen in $YSr_2Cu_{3-x}Mo_xO_{7+\delta}$ (5).

EXPERIMENTAL

$HoSr_2Cu_{2.7}Mo_{0.3}O_{7.54}$ was prepared from a stoichiometric mixture of the constituent oxides/carbonates (predried analytical grade Ho_2O_3, $SrCO_3$, CuO, and MoO_3) by high-temperature solid-state methods. The starting Cu : Mo molar ratio was 9 : 1 (2.7 : 0.3). The starting materials were weighed, ground to constant color, and fired in air in an alumina crucible, at 900°C for 24 hr. The sample was removed, reground and refired several times, and then pressed into a pellet for the final heat treatment. A preliminary X-ray powder pattern of the resulting, dense black powder indicated a clean tetragonal 123-type structure.

The oxygen content of $HoSr_2Cu_{2.7}Mo_{0.3}O_{7.54}$ was determined by thermogravimetric reduction under 5% hydrogen/nitrogen using a Dupont 951 thermobalance. The final temperature was 900°C. The calculated stoichiometry, assuming that the final products were Ho_2O_3, SrO, $SrMoO_4$ and Cu, is $HoSr_2Cu_{2.7}Mo_{0.3}O_{7.49(2)}$.

The composition of this doped Sr-123 phase was confirmed by electron microprobe analysis using a JEOL-JXA 8600 electron microprobe. Data were collected on polished $HoSr_2Cu_{2.7}Mo_{0.3}O_{7.54}$ specimens (1-μm^2 electron beam area, 15-kV accelerating voltage, 20-nA beam current). Reference standards of Ho metal, $SrTiO_3$, Cu_2O, and MoS_2 were used for determining the amount of Ho, Sr, Cu, and Mo, respectively. The average composition

[1] Present address: Department of Chemistry, Iowa State University, Ames, IA 50011.

0022-4596/95 $12.00

determined from five different samplings, normalized to 2 Sr per formula unit, was Ho : Sr : Cu : Mo = 1.04(2) : 2.0 : 2.66(6) : 0.30(1), in excellent agreement with the expected stoichiometry, based on mixing ratios of precursor phases. Trace amounts of unreacted holmium oxide were also observed.

An ~10-g sample of $HoSr_2Cu_{2.7}Mo_{0.3}O_{7.54}$ was sealed in a cylindrical vanadium sample can, and room-temperature [25(2)°C] time-of-flight (TOF) neutron powder data were collected on the SEPD diffractometer at Argonne National Laboratory. Using the ±145°, and ±90° detector banks, data were accumulated over an 8-hr period, corresponding to an approximate usable d-spacing range of 0.55–4.0 Å for the 145° bank, and 0.7–5.5 Å for the 90° bank. The data were collected and merged in the normal fashion, and a least-squares polynomial fit to a standard vanadium spectrum provided the parameters which describe the incident neutron spectral distribution for SEPD.

High-resolution powder X-ray data for $HoSr_2Cu_{2.7}Mo_{0.3}O_{7.54}$ (the same sample as used for the neutron diffraction experiment) were collected on an automated Scintag XDS 2000 diffractometer, using Cu$K\alpha$ radiation (λ = 1.5418 Å) for $20° < 2\theta < 100°$ (θ–θ scan; flat-plate sample geometry).

Initially, the $HoSr_2Cu_{2.7}Mo_{0.3}O_{7.54}$ neutron data alone were modeled by the Rietveld method, using the program GSAS (6). Typical starting atomic coordinates for an all-copper tetragonal 123-type structure were taken from the recent studies of $YSr_2Cu_{2.7}Mo_{0.3}O_7$ (4, 5). There was no evidence for a room-temperature orthorhombic distortion, or any superlattice peaks in $HoSr_2Cu_{2.7}Mo_{0.3}O_{7.54}$. Coherent neutron scattering lengths ($\times 10^{-12}$ cm) were assigned as follows: b(Ho) = 0.808, b(Sr) = 0.702, b(Cu) = 0.772, b(Mo) = 0.695, and b(O) = 0.581. The usual profile variables (scale factor, background polynomial coefficients, zero-point errors, peak-shape descriptors for each data bank, lattice parameters), and atomic parameters (positional and isotropic thermal factors) were refined to convergence, resulting in a satisfactory profile fit (profile residuals in the ~6% range). An absorption correction was successfully refined for each data bank.

Difference Fourier maps revealed that the O(1) species was split from its ideal (0, ½, 0) site to disordered (±x, ½, 0) positions, and O(1) was successfully modeled in this split configuration. The occupation of this site was also refined (*vide infra*). A very similar disordering effect of the equivalent oxygen atom was also observed in the studies of the $YSr_2Cu_{2.7}MoO_{0.3}O_7$ structure (4, 5). However, attempts at refining the Cu/Mo site populations of the nominal Cu(1) and Cu(2) sites for $HoSr_2Cu_{2.7}Mo_{0.3}O_{7.54}$ were inconclusive, and no reliable copper/molybdenum populations could be established for these sites from the neutron data alone. This lack of sensitivity probably results from the relative similarity in coherent neutron scattering lengths for Cu and Mo (0.772×10^{-12} and 0.695×10^{-12} cm, respectively). Refinements of the O(2), (0, ½, z) and O(3) (0, 0, z) site occupancies revealed insignificant change from full occupancy, and later refinement cycles fixed these values at unity.

In order to better characterize the Cu/Mo cation distribution over the chain [Cu(1)] and square-pyramidal [Cu(2)] sites, a joint time-of-flight neutron/X-ray Rietveld refinement was carried out using GSAS. This joint refinement strategy provides greater sensitivity in determining the copper/molybdenum distribution over the Cu(1) and Cu(2) sites (X-ray data), while maintaining the high sensitivity to oxygen-atom positions, occupancies, and thermal motions (neutron data). A similar joint powder neutron/X-ray refinement on $YBa_2Cu_3O_{7-\delta}$ (7) provided significant additional information on lattice vibrational modes in this material, compared to neutron-only measurements on the same phase.

With the powder X-ray data added to the refinement, the Cu/Mo site populations were optimized, subject to the constraint that the total Cu and Mo contributions to the Cu(1) and Cu(2) sites maintained a 9 : 1 ratio (i.e., the overall Cu : Mo ratio was maintained at 2.7 : 0.3, as synthesized, and in agreement with the microprobe data for $HoSr_2Cu_{2.7}Mo_{0.3}O_{7.54}$). This model immediately refined to stable and chemically reasonable Cu/Mo population values for both the Cu(1) and Cu(2) sites. Further refinement cycles modeled the thermal motion of all the atoms as anisotropic, resulting in a significant improvement in profile fit. At convergence, residuals of R_p = 4.21%, R_{wp} = 5.08%, and χ^2 = 2.45 were obtained. The final profile plot for the 90° neutron data is illustrated in Fig. 1, with the final X-ray data shown in Fig. 2. Crystallographic data for $HoSr_2Cu_{2.7}Mo_{0.3}O_{7.54}$ are summarized in Table 1.

As an additional check on the Cu/Mo site population result for $HoSr_2Cu_{2.7}Mo_{0.3}O_{7.54}$, further refinements were carried out with fixed Cu/Mo distributions over the nominal Cu(1) and Cu(2) sites. A model which placed all the molybdenum at the square-pyramidal Cu(2) site (similar to the results of Hu *et al.* (4) for $YSr_2Cu_{2.7}Mo_{0.3}O_7$) resulted in slightly poorer overall residuals of R_p = 4.22%, R_{wp} = 5.15%, and χ^2 = 2.52. The individual R factors for the two neutron histograms were similar to the "free" $HoSr_2Cu_{2.7}Mo_{0.3}O_{7.54}$ refinement described above, but the residuals (R_p = 4.17%, R_{wp} = 6.13%) for the X-ray data were the most affected by this change in Cu/Mo distribution. A model similar to the results of Harlow *et al.* (5) for $YSr_2Cu_{2.7}Mo_{0.3}O_7$ [all Mo substitutes at the Cu(1) site] also refined to slightly higher disagreement factors: R_p = 4.22%, R_{wp} = 5.14%, and χ^2 = 2.51. Once again, the fit to the X-ray data was most affected by this change in molybdenum/copper occupancies: X-ray R_p = 4.16%, X-ray R_{wp} = 6.11%. A comparison of "extracted structure factor" [$R(F^2)$] residuals for the X-ray data bank confirms

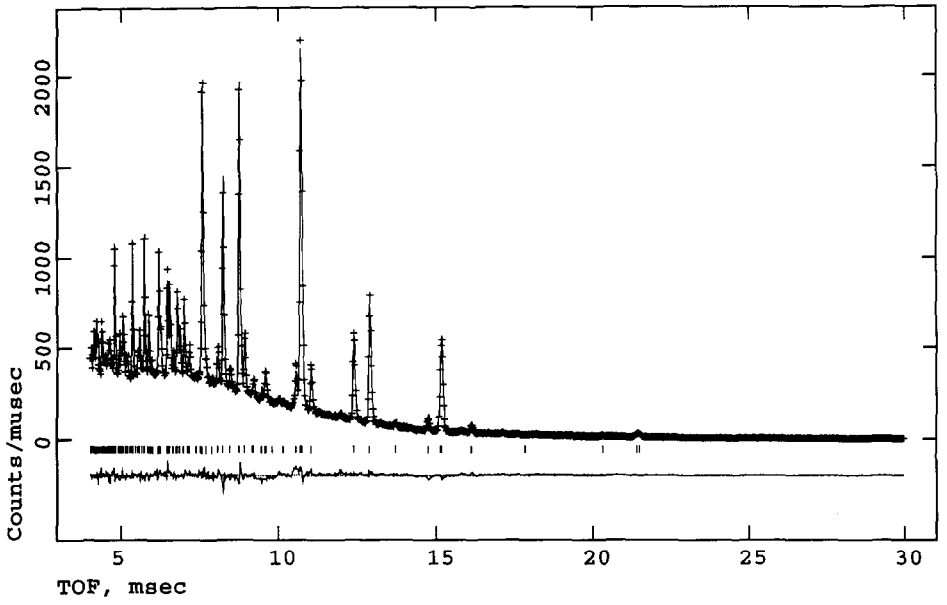

FIG. 1. Final observed (crosses), calculated (line), and difference profiles for the 90° scattering angle time-of-flight neutron data for $HoSr_2Cu_{2.7}Mo_{0.3}O_{7.54}$. Allowed reflection positions are indicated by vertical tick marks.

this pattern for the three refinements: $R(F^2)$ for the as-refined model = 7.74%; $R(F^2)$ for the molybdenum at Cu(2) site model = 8.06%; and $R(F^2)$ for the molybdenum at Cu(1) site model = 8.02%.

RESULTS AND DISCUSSION

$HoSr_2Cu_{2.7}Mo_{0.3}O_{7.54}$ crystallizes as the tetragonal ($P4/mmm$) modification (8) of the $YBa_2Cu_3O_{7-\delta}$ high-T_c superconductor structure. Final atomic positional and thermal parameters for $HoSr_2Cu_{2.7}Mo_{0.3}O_{7.54}$ are listed in Table 2, and selected geometrical data are reported in Table 3. The $HoSr_2Cu_{2.7}Mo_{0.3}O_{7.54}$ structure is illustrated in Fig. 3.

There are two main points of interest in this particular modification of this familiar structural type (1, 4, 5): First, we note that the substitution of molybdenum for copper occurs at both Cu sites in the structure to a similar extent;

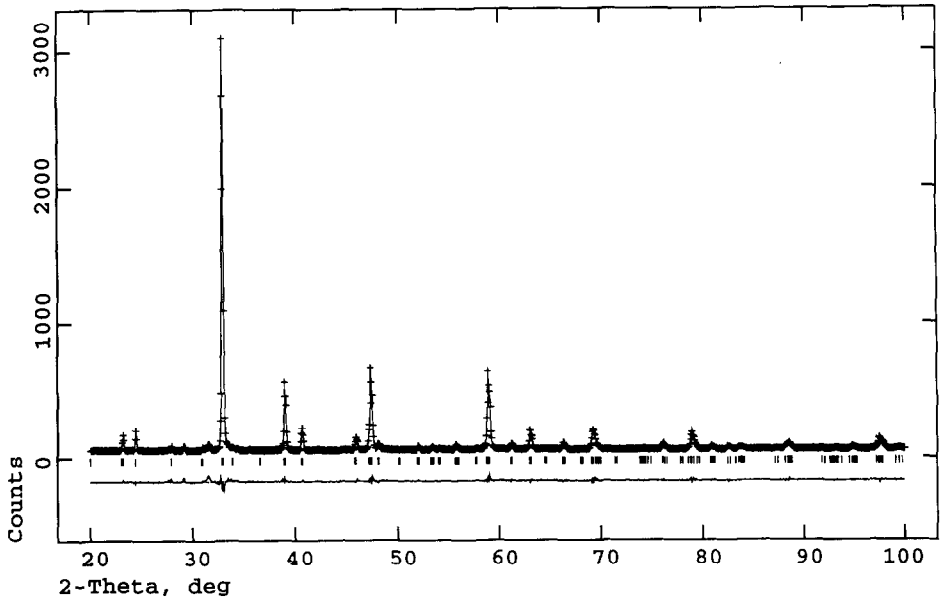

FIG. 2. Final observed (crosses), calculated (line), and difference profiles for the powder X-ray data for $HoSr_2Cu_{2.7}Mo_{0.3}O_{7.54}$. Allowed reflection positions are indicated by vertical tick marks.

TABLE 1
Crystallographic Parameters for $HoSr_2Cu_{2.7}Mo_{0.3}O_{7.54}$

Formula wt.	660.51
Habit	Black powder
Crystal system	Tetragonal
a (Å)	3.83107(6)
c (Å)	11.5347(3)
V (Å^3)	169.296(8)
Space group	$P4/mmm$ (No. 123)
Z	1
T (°C)	25(1)
ρ_{calc} (g/cm^3)	6.48
No. of variables	61
No. of data	10910
R_p, R_{wp} (%)[a]	4.59, 4.25
R_p, R_{wp} (%)[b]	3.54, 4.96
R_p, R_{wp} (%)[c]	4.06, 5.98
R_p, R_{wp} (%)[d]	4.21, 5.08
χ^2 (overall)	2.45

[a] 145° TOF neutron data bank.
[b] 90° TOF neutron data bank.
[c] X-ray data.
[d] Overall residuals.

12.2(5)% Mo occupies the Cu(1) site, and 7.8(5)% Mo substitutes for Cu(2).

The Cu(2) site is coordinated by five oxygen atom neighbors in square-pyramidal configuration (Table 3), with a typical, long apical distance [2.272(3) Å], and four shorter in-plane Cu/Mo–O contacts [1.9241(2) Å]. The copper atom is displaced from the plane of its four in-plane neighbors by ~0.18 Å, toward the apical oxygen atom, thus, the Cu(2)/O(2) planes are distinctly puckered, which may be significant with respect to the superconducting properties of this phase. This Cu/Mo(2) coordination may be compared with that observed in $YSr_2Cu_3O_7$ itself (1.916 Å for the in-plane bonds, and 2.343 Å for the apical bond) (1). The second, "chain" copper site [Cu(1)] shows considerable thermal motion in the ab-plane (Table 2, Fig. 4), with $U_{11} = U_{22} > U_{33}$. This may well represent a static displacement in the xy-plane of this Cu/Mo atom from its ideal (0, 0, 0) site: A similar effect was observed for $YSr_2Cu_{2.7}Mo_{0.3}O_7$ (5).

The second significant structural feature in $HoSr_2Cu_{2.7}Mo_{0.3}O_{7.54}$ concerns the O(1) species, which is disordered from its ideal (0, ½, 0) position in this structure type to a (±x, ½, 0) site, with x = 0.179 (9): The apparent O(1) ··· O(1) separation is 1.41(2) Å. The O(1) thermal motion in the ab-plane is extremely large (Fig. 4), which is consistent with the probable Cu/Mo(1) displacement from its ideal site. This disorder might be rationalized as a consequence of the different preferred local coordinations of the copper (planar) and molybdenum (distorted octahedral) atoms at the adjacent disordered metal site. Alternately, a (local) "concerted rotation" of nominal octahedra may occur to optimize the strontium–oxygen coordination environment.

TABLE 2
Atomic Positional/Thermal Parameters for $HoSr_2Cu_{2.7}Mo_{0.3}O_{7.54}$

Atom	W[a]	x	y	z	U_{eq} (Å^2)
Ho(1)	1d	½	½	½	0.0037
Sr(1)	2h	½	½	0.1971(1)	0.0181
Cu(1)[b]	1a	0	0	0	0.0322
Cu(2)[c]	2g	0	0	0.3583(2)	0.0059
O(1)[d]	4n	0.183(3)	½	0	0.1146
O(2)	4i	0	½	0.3740(1)	0.0103
O(3)	2g	0	0	0.1613(2)	0.0311

	U_{11}	U_{22}	U_{33}	U_{12}	U_{13}	U_{23}
Ho(1)	0.0034(5)	0.0034(5)	0.0042(7)	0	0	0
Sr(1)	0.0192(6)	0.0192(6)	0.0159(8)	0	0	0
Cu(1)	0.0444(9)	0.0444(9)	0.008(2)	0	0	0
Cu(2)	0.0024(4)	0.0024(4)	0.0128(7)	0	0	0
O(1)	0.179(9)	0.156(8)	0.008(4)	0	0	0
O(2)	0.0072(5)	0.0029(5)	0.0207(7)	0	0	0
O(3)	0.040(1)	0.040(1)	0.014(2)	0	0	0

[a] Wyckoff site.
[b] Refined fractional site occupancies: Cu 0.878(5), Mo 0.122(5).
[c] Refined fractional site occupancies: Cu 0.922(5), Mo 0.078(5).
[d] Refined fractional site occupancy: 0.386(9) (disordered with respect to (0, ½, 0) site.

TABLE 3
Selected Bond Distances (Å)/Angles (°) for $HoSr_2Cu_{2.7}Mo_{0.3}O_{7.54}$

Ho(1)–O(2) × 8	2.4043(7)	Sr(1)–O(1)[a] × 4	2.577(4)
Sr(1)–O(2) × 4	2.799(2)	Sr(1)–O(3) × 4	2.7403(4)
Cu(1)–O(1)[a] × 2	2.040(3)	Cu(1)–O(3) × 2	1.860(3)
Cu(2)–O(2) × 4	1.9241(2)	Cu(2)–O(3)	2.272(3)
O(2)–Cu(2)–O(2)	169.2(2)	O(2)–Cu(2)–O(2)	89.49(2)
O(2)–Cu(2)–O(3)	95.42(6)	Cu(1)–O(1)[a]–Cu(1)	139.8(4)
Cu(2)–O(2)–Cu(2)	169.2(2)	Cu(1)–O(3)–Cu(2)	180

[a] The O(1) species is partially occupied (Table 2).

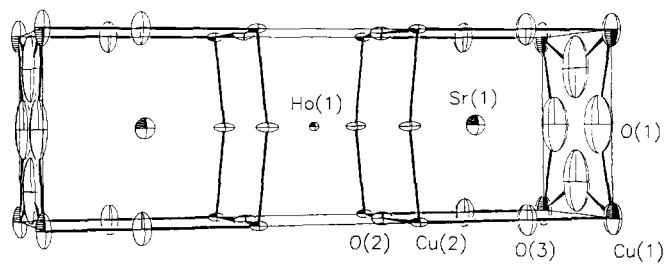

FIG. 3. View of the $HoSr_2Cu_{2.7}Mo_{0.3}O_{7.54}$ crystal structure, with selected atoms labeled.

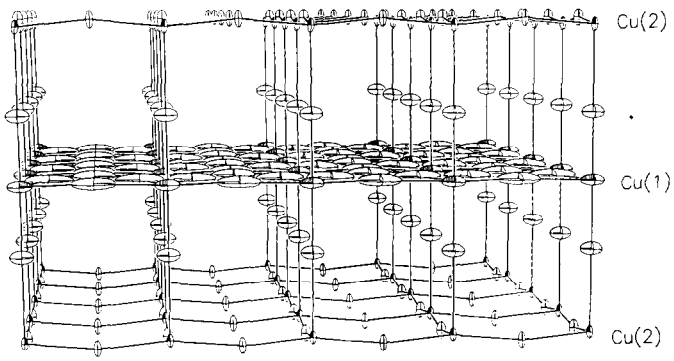

FIG. 4. View of an *ab*-slab of the $HoSr_2Cu_{2.7}Mo_{0.3}O_{7.54}$ crystal structure showing the disordered Cu/Mo(1)/O(1) planes (see text). Ho and Sr species are omitted for clarity.

The refined O(1) partial site occupancy, 0.386 (9), results in an overall oxygen stoichiometry of 7.54 for this phase, which is in excellent agreement with the value of 7.49 (2) obtained from the chemical analysis measurement. Assuming that the molybdenum enters the structure as Mo^{VI}, and the other atoms maintain their normal, stable oxidation states (Ho^{III}, Sr^{II}, O^{II-}), then the average copper valence over the Cu(1) and Cu(2) sites in this structure is +2.32. We note that the average Cu valence in $YBa_2Cu_3O_{7-\delta}$ ($\delta \approx 0$) of +2.33 is almost identical to the value found for this tetragonal strontium 123 phase.

The crystallochemical environments of the holmium and strontium atoms are typical for this class of material. The interlayer Ho(1) cation is 8-coordinated by nearby O(2) atoms, and separates adjacent Cu(2)/O(2) sheets. A bond valence sum (BVS) of 2.85 (expected 3.00) results for holmium (9). The Sr(1) cation is bonded to a nominal 4 × O(1), 4 × O(2), and 4 × O(3) (Table 3). Because the O(1) site is only 39% occupied, the average Sr coordination over the entire structure is 9.6 oxygen atoms, and assuming this number, a BVS[Sr(1)] of 1.83 results (expected 2.00), with d_{av}(Sr–O) = 2.705 Å. A Cu(2) · · · Cu(2) interlayer separation of 3.269 Å is found in $HoSr_2Cu_{2.7}Mo_{0.3}O_{7.54}$ [3.353 Å for $YSr_2Cu_{2.7}Mo_{0.3}O_7$ (5)].

In conclusion, the detailed crystal structure of the high-T_c superconductor $HoSr_2Cu_{2.7}Mo_{0.3}O_{7.54}$ has been investigated by a joint neutron/X-ray profile refinement, which yielded more detail than either of the two techniques alone. A reliable estimate of the total oxygen content and Cu/Mo distribution over each copper site was obtained, as well as information on the anisotropic thermal motion/disorder of the oxygen atoms in this structure. On the evidence presented here, $HoSr_2Cu_{2.7}Mo_{0.3}O_{7.54}$ appears to have a different Cu/Mo cation distribution than that found in $YSr_2Cu_{2.7}Mo_{0.3}O_7$ (4, 5).

ACKNOWLEDGMENTS

We thank M. A. Subramanian (Dupont) for sharing his results of $YSr_2Cu_{2.7}Mo_{0.3}O_7$ with us, prior to publication. J. K. Meen (Texas Center for Superconductivity) collected the electron microprobe data, and R. L. Hitterman (Argonne National Laboratory) collected the neutron data for $HoSr_2Cu_{2.7}Mo_{0.3}O_{7.54}$. This work is partially funded by the National Science Foundation (DMR9214804) and the Welch Foundation.

REFERENCES

1. B. Okai, *Jpn. J. Appl. Phys.* **29,** L2180 (1990).
2. Q. Xiong, Y. Q. Wang, J. W. Chu, Y. Y. Sun, K. Matsuishi, H. H. Feng, P. H. Hor, and C. W. Chu, *Physica C* **198,** 70 (1992).
3. P.-H. Hor, J. W. Chu, X. Q. Wang, H. H. Feng, Y. Y. Sun, K. Matsuishi, Q. Xiong, and C. W. Chu, *in* "HTS Materials, Bulk Processing and Bulk Applications" (C. W. Chu, W. K. Chu, P.-H. Hor, and K. Salama, Eds.), pp. 53–57. World Scientific, Singapore, 1992.
4. S. F. Hu, R. S. Liu, S. C. Su, D. S. Shy, and D. A. Jefferson, *J. Solid State Chem.* **112,** 203 (1994).
5. R. L. Harlow, G. H. Kwei, R. Suryanarayanan, and M. A. Subramanian, *Physica C*, in press (1995).
6. A. C. Larson and R. B. Von Dreele, "GSAS User Guide." Los Alamos National Laboratory, New Mexico, 1990.
7. A. Williams, G. H. Kwei, R. B. Von Dreele, A. C. Larson, I. D. Raistrick, and D. L. Bish, *Phys. Rev. B* **37,** 7960 (1988).
8. W. I. F. David, W. T. A. Harrison, R. M. Ibberson, M. T. Weller, J. R. Grasmeder, and P. Lanchester. *Nature (London)* **328,** 328 (1987).
9. N. E. Brese and M. O'Keeffe *Acta. Crystallogr. Sect. B* **47,** 192 (1991).